

the hardening of the amphoteric gel matrix, while the decrease of cross-linking density causes softening.

Amphoteric gels we have investigated contain both negatively and positively charged atomic groups, $-\text{COO}^-$ and $-\text{NH}_3^+$. They form a salt linkage, $-\text{COO}^- \cdots ^+\text{H}_3\text{N}-$. So the hardness variation of amphoteric gels is primarily an electrostatic effect. Therefore the potential behavior within the gel must reflect the hardness behavior of amphoteric gels.

In this study, we performed potential measurement within neutral, anionic, cationic, and amphoteric gels along with measurement of their swelling ratios. We also performed quantitative measurement of their hardness, since our previous investigation went no further than qualitative measurement. Then we discussed the gel-hardening phenomenon through examination of the correlation between the potential and the hardness of gels.

2. Materials and methods

Basically four types of acrylamide-based gels—neutral, anionic, cationic, and amphoteric gels—were prepared, all plate-shaped. Further, as to anionic and amphoteric gels, five different types of anionic gels and four different types of amphoteric gels were prepared. The chemicals employed to prepare these gels are summarized in Table 1 along with their notations. Acrylamide and *N,N*-methylenebisacrylamide were purchased from Wako (Osaka, Japan). Acrylic acid, *N,N,N',N'*-tetramethylethylenediamine, and ammonium persulfate were purchased from Kishida (Osaka, Japan), and allylaminehydrochloride was purchased from TCI (Tokyo, Japan).

The chemicals were dissolved in deionized water and poured into the plate-shaped mold. The solution was heated at 65 °C for 1 h. It has been known that the $-\text{CONH}_2$ atomic group of the acrylamide molecule can be hydrolyzed into a $-\text{COOH}$ atomic group in highly concentrated NaOH solution [2–5]. Thus, four anionic gels—AN1, AN5, AN48, AN72—were prepared through the immersion of neutral gels, N0, in 1 M NaOH solution for 1, 5, 48, and 72 h, respectively. All of the amphoteric gels—AM1, AM5, AM48, AM72—were prepared through the immersion of cationic gels, CA0, in 1 M NaOH solution for 1, 5, 48, and 72 h, respectively. On the completion of synthesis, the gels were washed by

repetitive immersion in deionized water and acetone alternately. Then they were all stored in deionized water until they reached the equilibrium state. The deionized water was replaced with new water at least once a day for 5 days, since ionic gels release ions and change the bathing deionized water condition, causing significant property changes of gels.

2.1. Potential measurement

We performed potential measurement on the gels. An Ag/AgCl electrode was stuck into the gel matrix, while counter Ag/AgCl electrode was placed in the bathing solution. The potential within the gel with respect to the potential of the bathing solution was measured using an HE-104 electrometer (HIOKUTO DENKO Corp., Tokyo, Japan) in the manner depicted in Fig. 1. This experiment was performed under the atmosphere at room temperature.

2.2. Hardness measurement

Gel hardness is usually assessed by the use of a rheometer. However, access to rheometers is not easy, since they are not a commonly or widely used apparatus. On the other hand, Hertz contact theory is a quite simple method for hardness assessment on material in the static state [6]. We employed this theory to assess the gel hardness. This experiment was performed under the atmosphere at room temperature.

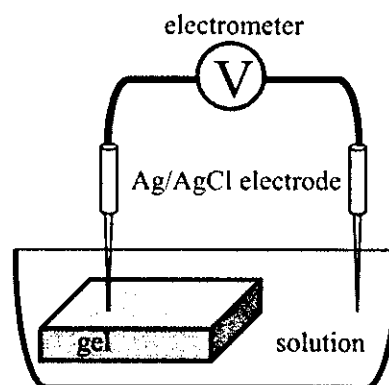


Fig. 1. Potential measurement setup. An Ag/AgCl electrode is stuck into a gel, and the Ag/AgCl counterelectrode is placed in the solution.

Table 1
The chemical weights employed for gel processing

Notation	AAm (g)	AAc (g)	AAHC (g)	MBA (g)	TEMED (g)	AP (g)	DW (g)
N0	11.56	0.00	0.00	0.154	0.10	0.08	100
AN0	8.52	2.87	0.00	0.154	0.10	0.08	100
CA0	8.52	0.00	3.72	0.154	0.10	0.08	100

Notes. N0, neutral gel; AN0–AN72, anionic gels; CA0, cationic gel; AM1–AM72, amphoteric gels; AN1–AN72 and AM1–AM72 were prepared through the hydrolysis of N0 and CA0, respectively, in 1 M NaOH solution for 1, 5, 48, and 72 h. AAm: acrylamide. AAc: acrylic acid. AAHC: allylaminehydrochloride. MBA: *N,N*-methylenebisacrylamide. TEMED: *N,N*-tetramethylethylenediamine. AP: ammonium persulfate. DW: deionized water.

Table 2
The potential, V , and swelling ratio, SR, of gels

	SR	V (mV)
N0	2.32	-10.88
AN0	11.72	-58.5
AN1	74.75	-56.2
AN5	112.85	-64.2
AN48	90.57	-59.9
AN72	103.18	-61.4
CA0	19.13	+26.5
AM1	36.5	-57.5
AM5	55.4	-57.2
AM48	96.9	-60.1
AM72	95.8	-59.4

Notes: Swelling ratio, SR, is defined by $SR = [(thickness\ of\ water\ swollen\ gel)/(thickness\ of\ gel\ right\ after\ its\ synthesis)]^3$.

3. Results and discussion

3.1. Gel potential

Table 2 shows the potential and swelling ratio of gels, where their swelling ratio, SR, is defined by $SR = [(thickness\ of\ water\ swollen\ gel)/(thickness\ of\ gel\ right\ after\ its\ synthesis)]^3$. Neutral, anionic, and cationic gel potentials are almost neutral, negative, and positive, respectively. This suggests that the sign of the potential within the gels is determined by the sign of the fixed charge contained in them. The anionic gel contains the fixed negative charge of $-COO^-$, causing a negative potential, while the cationic gel contains the fixed positive charge of $-NH_3^+$, causing a positive potential. The neutral gel, N0 contains no fixed charges and its potential, -10.88 mV, is the closest to 0 mV among all the gels.

What attracts our attention is that the potentials of AN0–AN72 are maintained constant at ~ -60 mV, although their chemical compositions and the processing procedures are different and their swelling ratios are different, too. This suggests that the charge density in these gels is the almost same regardless of their swelling ratios. This can be easily explained by a commonly known concept of the chemical reaction. The reaction



occurs in the anionic gels.

Since the dissociation constant of this chemical reaction is constant as long as the environmental temperature is constant, the concentrations of $-COOH$, $-COO^-$, and H^+ contained in the five anionic gels, AN0–AN72, should be constant. Therefore the charge densities of $-COO^-$ atomic groups are the same, causing the same potential, although the swelling ratios are different due to the different amounts of $-COOH$ created in AN0–AN72.

In order to fully confirm the potential maintenance of ~ -60 mV for the anionic gels regardless of their swelling ratio, we performed the following experiment: Nakano et al.

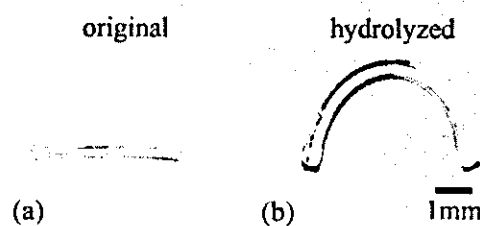


Fig. 2. Gel curving. The nonhydrolyzed straight acrylicamide gel in photo (a) curves as shown in photo (b) through the hydrolysis of its upper part.

reported that the plate-shaped acrylicamide gel can be brought into a curved shape in the equilibrium swollen state in deionized water as depicted in Fig. 2 by locally hydrolyzing the gel matrix [7]. This gel was originally a straight neutral gel; then only the top layer of it was hydrolyzed significantly in 0.1 M NaOH solution (see Fig. 2 again). The top layer came to have $-COOH$ groups, which have a high affinity to water molecules. Therefore once this gel was immersed in the deionized water, it swelled with different degrees of swelling ratio along its thickness, causing the gel-shape to curve as in Fig. 2. Namely, the swelling ratio increases from the bottom layer toward the top layer. We applied this method to the anionic gel, AN0. Three different types of AN0 whose top layer was hydrolyzed in 0.1 M NaOH solution for 10, 20, and 30 min, respectively, were prepared, and they were designated as AN0-10, AN0-20, and AN0-30, respectively. Since the intact AN0 originally contained $-COOH$ groups, all of AN0-10, AN0-20, and AN0-30 contain enough $-COOH$ to generate a negative potential at least reaching ~ -60 mV. They were immersed in the deionized water, and all of them deformed into the curved shape. After they reached equilibrium, the potential behavior within them along their thickness direction was probed by sticking Ag/AgCl electrodes into their gel matrix, where the Ag/AgCl counterelectrode was placed in the deionized water bathing them. We observed the virtually constant potentials for all of AN0-10, AN0-20, and AN0-30, regardless of the electrode tip depth from the gel top surface. Potential deviation was within only about 1 mV, even when the electrode tip depth was displaced by a few mm. Therefore undoubtedly the constant potential is realized through the maintenance of a constant charge density of $-COO^-$, resulting in a swelling ratio change. This strongly suggests that the potentials AN0–AN72 are maintained constant at ~ -60 mV autonomously.

We have to add some comments on this measurement. From our investigation, the potentials within AN0-10, AN0-20, and AN0-30 virtually did not deviate. However, in the extreme vicinity of these gels' top and bottom surfaces within their matrices, the potentials decay by a few tens of mV. This could be explained by the concept put forward by Ling [8–11]. Ling suggested that injury to biological cells disturbs the activity of ions in the cell. This gives rise to a cell potential disturbance. Since the nature of the gel has been considered to be quite similar to that of a cell, this concept

of potential disturbance in the cell injury must be applicable as the cause of the gel potential decay. The surfaces of AN0-10, AN0-20, and AN0-30 are undoubtedly directly exposed to the external bathing solution, not protected by the rest of gel matrix. So their surfaces are continuously attacked by the bombardment of the surrounding water molecules. This must cause a potential disturbance of the gel at the surface, causing potential decay.

Regarding amphoteric gels, AM1–AM72, all of them exhibit negative potentials, although their starting materials are the same cationic gel, CA0, which exhibited the positive potential in Table 2. This suggests that $-\text{COOH}$ created in amphoteric gels through their hydrolysis dominates the potential generation rather than $-\text{NH}_2$. In fact, their potentials are virtually constant, ~ -60 mV, which is the same as those of AN0–AN72 containing $-\text{COOH}$ atomic groups, although their large swelling ratio difference goes to about 2.5-fold. To explain this phenomenon, we can speculate that the concentrations of $-\text{COOH}$, $-\text{COO}^-$, and H^+ in AM1–AM72 are constant, regardless of their swelling ratios, just like AN0–AN72, described in Section 3.1. Besides that, the swelling ratio behavior of amphoteric gel, for instance AM5, in the pH solutions is quite similar to that of anionic gel, AN0, as shown in Figs. 3a and 3c. Both AM5 and AN0 exhibit quite large swelling ratios in the high-pH solutions and quite small swelling ratios in the low-pH solutions. This suggests the occurrence of the reactions $-\text{COOH} \rightarrow -\text{COO}^- + \text{H}^+$ in the high-pH solutions and $\text{COOH} \leftarrow \text{COO}^- + \text{H}^+$ in the low-pH solutions for both gels, since $-\text{COOH}$ has a preventive effect on gel swelling due to the formation of hydrogen bonds and $-\text{COO}^-$ has a promotional effect on gel swelling due to the high affinity of its charge to the water molecules. Therefore $-\text{COOH}$ rather than $-\text{NH}_2$ is the predominant atomic group for the potential behavior of amphoteric gels. In addition to this, the swelling ratio behavior of cationic gels containing $-\text{NH}_2$ atomic groups, CA0, is totally different from that of AM5, as shown in Fig. 3b. CA0 exhibits a large swelling in the low-pH solutions.

3.2. Gel hardness

The Young's moduli of gels, E_{gel} , was evaluated by employing the Hertz contact theory [6]. We placed several different sizes and weights of quite hard ceramic balls on the plate-shaped gels and measured the depth of the hollow, D_{gel} , created by these balls on the gel surfaces (see Fig. 4). The radius of the contact area between the gel and the ball, R_{contact} , is given by the simple calculation $R_{\text{contact}} = (2R_{\text{ball}}D_{\text{gel}} - D_{\text{gel}}^2)^{1/2}$, where R_{ball} is the radius of the ball placed on the gel surface (see Fig. 4). According to the Hertz contact theory, the relationship between the gel Young's modulus and the contact area radius is given by

$$R_{\text{contact}}^3 = (3/4)R_{\text{ball}} \left[(1 - \nu_{\text{ball}}^2)/E_{\text{ball}} + (1 - \nu_{\text{gel}}^2)/E_{\text{gel}} \right] \times (W_{\text{ball}}g), \quad (2a)$$

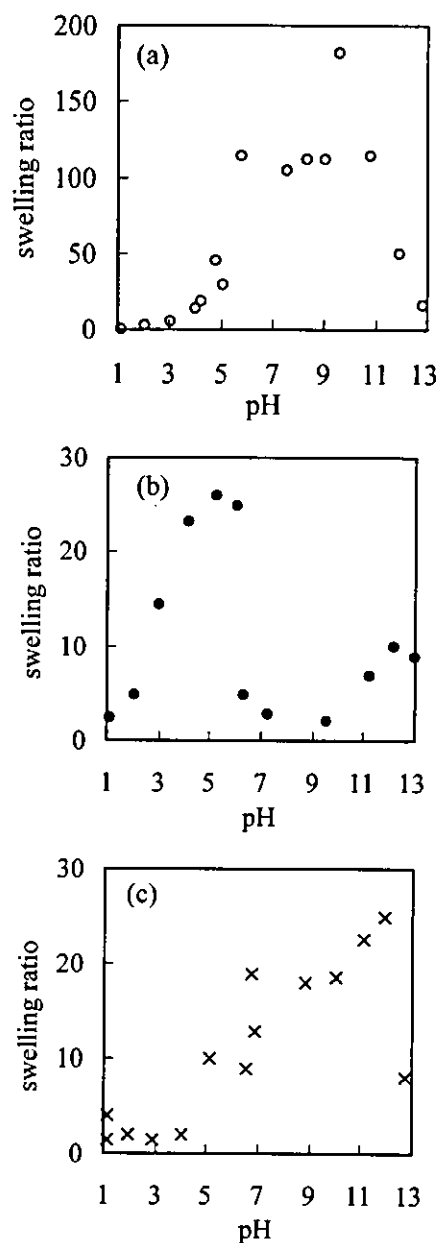


Fig. 3. pH dependence of gel swelling ratio: (a) AN0, (b) CA0, (c) AM5.

where E_{ball} , ν_{ball} , and W_{ball} are the Young's modulus, Poisson ratio, and weight of the ceramic ball, respectively, and ν_{gel} and g are the Poisson ratio of the gel and the gravitational acceleration, respectively. Under the assumptions $E_{\text{ball}} \gg E_{\text{gel}}$ and $\nu_{\text{gel}} = 1/2$. Eq. (2a) is simplified and rearranged into

$$R_{\text{contact}}^3 = (9/16)(R_{\text{ball}}W_{\text{ball}}g)/E_{\text{gel}}. \quad (2b)$$

From Eq. (2b), the Young's moduli of all gels were calculated. Table 3 shows the Young's moduli of gels. Young's moduli of AN1–AN72 are all less than that of N0. AN1–AN72 were prepared through the hydrolysis of N0; that is, their major structures are basically the same. However,

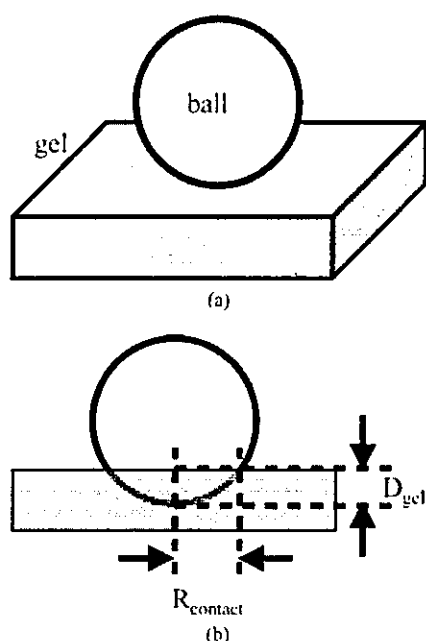


Fig. 4. Schematic illustration of hardness measurement on the gels: (a) overhead view; (b) side view.

Table 3
The Young's modulus, E_{gel} , of gels

	E_{gel} (MPa)
N0	0.012
AN0	0.006
AN1	0.011
AN5	0.008
AN48	0.011
AN72	0.008
CA0	0.005
AM1	0.011
AM5	0.010
AM48	0.007
AM72	0.008

the amounts of $-\text{COOH}$ contained in them are strongly speculated to be different from one another because of their different duration of hydrolysis. Therefore the smaller Young's modulus of AN1–AN72 than N0 must be due to the larger swelling ratio of AN1–AN72 compared with N0. Their swelling ratios are about several tens of N0. Namely, the molecular network densities of AN1–AN72 are several tenths of N0, resulting in their lower Young's moduli. One may think that it is against his or her intuition that the Young's modulus of N0 is not significantly smaller than those of AN1–AN72, despite the observation of the extremely smaller swelling ratio of N0 than of AN1–AN72. The following is our answer to this question: Although we have not identified what causes this phenomenon exactly, we strongly suspect the formation of additional cross-linkings hydrogen bonds between $-\text{COOH}$ s contained in AN1–AN72, and they could reinforce their matrices com-

parably to the hardness of N0. Although the duration times of hydrolysis of AN1–AN72 are different from one another, which creates the different amounts of $-\text{COOH}$ contained in AN1–AN72, there was not such significant differences among their Young's moduli. It also can be explained through the creation of hydrogen bondings and the maintenance of the constant concentration of $-\text{COOH}$ as described in Section 2.1. Namely, regardless of the swelling ratio, the density of cross-linking hydrogen bonds was maintained constant. Therefore as long as the hardness of AN1–AN72 is dominated primarily by the hydrogen bonds, their Young's moduli could be maintained almost constant regardless of their swelling ratio. This explanation is quite consistent with the discussion in Section 2.1.

AM1–AM72 were prepared through the hydrolysis of CA0; that is, their major structures are basically the same. However, the amounts of $-\text{COOH}$ contained in them are strongly speculated to be different because of the different duration time of hydrolysis and their large variation of swelling ratio (see Table 2). Young's moduli of AM1 and AM5 are about twofold CA0's Young's modulus. However, the swelling ratios of AM1 and AM5 are both two- to threefold larger than that of CA0. Namely, the molecular network densities of AM1 and AM5 are both lower than that of CA0, yet still their Young's moduli are larger than that of CA0. As was reported before, this phenomenon was speculated to be caused by the formation of intramolecular salt linkages between $-\text{COOH}$ and $-\text{NH}_2$, $-\text{COO}^- \cdots +\text{H}_3\text{N}-$ [3,4]. Salt linkages serve as additional cross-linkings reinforcing the matrices of AM1 and AM5. The swelling ratios of AM48 and AM72 are much larger than that of CA0, yet still their Young's moduli are larger than CA0. This suggests that the gel matrix reinforcement by the salt linkages is quite effective. AM48 and AM72 have the larger swelling ratios and the smaller Young's moduli than AM1 and AM5. This must be due to the creation of larger amounts of $-\text{COOH}$ in AM48 and AM72 than in AM1 and AM5 due to the longer hydrolysis duration of AM48 and AM72 than of AM1 and AM5. Namely, the larger amount of $-\text{COO}^-$ must exist through the dissociation of a larger amount of $-\text{COOH}$ in AM48 and AM72; thus AM48 and AM72 swell until their fixed charge density of $-\text{COO}^-$ is the same as those of AM1 and AM5. In other words they swelled until the potential of ~ -60 mV was realized. This resulted in larger swelling ratios of AM48 and AM72 than of AM1 and AM5 and led to lower molecular network densities (or smaller Young's moduli) of AM48 and AM72 than of AM1 and AM5. Concerning this point, one question may be raised: that AM48 and AM72 have a higher opportunity to form salt linkages, compared with AM1 and AM5, because of the presence of more $-\text{COOH}$ in them than in AM1 and AM5, so that the Young's moduli of AM48 and AM72 should be larger than those of AM1 and AM5. In spite of this plausible speculation, smaller Young's moduli of AM48 and AM72 than of AM1 and AM5 were observed. This could be explained by the lack of the counterpart of $-\text{COO}^-$, that is, $-\text{NH}_3^+$, to form salt linkages in

AM48 and AM72. All of AM1, AM5, AM48, and AM72 definitely have the same amount of $-\text{NH}_2$ in their bodies. In the swollen state, some $-\text{NH}_2$ is converted into $-\text{NH}_3^+$, which can serve as a counterpart of $-\text{COO}^-$ for the formation of a salt linkage. Although AM48 and AM72 contain larger numbers of $-\text{COO}^-$, the number of $-\text{NH}_3^+$ is limited. Therefore the increase in the number of $-\text{COO}^-$ cannot infinitely increase the number of salt linkages. So the presence of the excess $-\text{COO}^-$ that cannot get involved in salt-linkage formation in AM48 or AM72 merely further promotes the absorption of water molecules in their bodies, resulting in their larger swelling ratios. The larger swelling ratio without the increase of the number of salt linkages merely lowers the molecular network density. Therefore the Young's moduli of AM48 and AM72 are smaller than those of AM1 and AM5.

4. Summary and conclusions

Amphoteric gel characteristics of swelling ratio, potential, and hardness were quantitatively evaluated and these characteristics were found to be under greater influence by $-\text{COOH}$ groups than by $-\text{NH}_2$. These results are regarded as strong supportive evidence that the participation of $-\text{COO}^-$ created through the dissociation of $-\text{COOH}$ in the formation of salt linkages has a predominant role in the hardness variation of amphoteric gels. Additionally, we speculated that the hydrogen bonds between $-\text{COOH}$ s could also reinforce the anionic gel matrix to a large extent.

Acknowledgments

This research was conducted under the financial support of Health and Labor Science Research Grants of Research on Advanced Medical Technology (No. H14-nano-021) from the Ministry of Health Labor and Welfare and the Mikiya Science and Technology Foundation, both in Japan.

References

- [1] T. Tanaka, *Sci. Am.* 244 (1981) 124.
- [2] Y. Osada, S.B. Ross-Murphy, *Sci. Am.* 268 (1993) 82.
- [3] H. Tamagawa, F. Nogata, S. Umemoto, N. Okui, S. Popovic, M. Taya, *Bull. Chem. Soc. Jpn.* 75 (2002) 383.
- [4] H. Tamagawa, F. Nogata, T. Watanabe, A. Abe, J.-Y. Jin, S. Popovic, M. Taya, *JSME Int. J. A* 45 (2002) 579.
- [5] A. Shozawa, Master's thesis, Tokyo Institute of Technology, 1987.
- [6] I. Nakahara, *Zairyourikigaku [Strength of Material]*, Yokendo, Tokyo, 1976 [in Japanese].
- [7] T. Nakano, T. Tamagawa, T. Noagata, S. Ishihara, preprint, JSME Conference, 2001.
- [8] G.N. Ling, *In Search of the Physical Basis of Life*, Plenum, New York/London, 1984.
- [9] G.N. Ling, *A Revolution in the Physiology of the Living Cell*, Krieger, 1992.
- [10] G.N. Ling, *Life at the Cell and Below-Cell Level: The Hidden History of a Fundamental Revolution in Biology*, Pacific Press, New York, 2001.
- [11] G.N. Ling, *Physiol. Chem. Phys. Med. NMR* 29 (1997) 123.



Bending response of dehydrated ion exchange polymer membranes to the applied voltage

H. Tamagawa*, F. Nogata

*Department of Human and Information Systems, Faculty of Engineering, Gifu University,
1-1 Yanagido, Gifu 501-1193, Japan*

Received 15 March 2004; accepted 21 June 2004

Available online 26 August 2004

Abstract

Ion exchange polymer membrane in the dehydrated state was found to exhibit bending upon a small applied voltage, although the investigations on the hydrated ion exchange polymer membrane bending behavior have been performed quite intensively for more than a decade for the purpose of producing a practical polymer actuator. Our investigation on the dehydrated ion exchange polymer membrane has revealed that its bending direction is perfectly controllable by the polarity control of applied voltage and the degree of its bending curvature is also almost completely determined by the control of duration time of voltage application on it, while the hydrated ion exchange polymer membranes lack of such properties. Furthermore, the longevity of dehydrated ion exchange polymer membrane sustaining such a highly controllable properties has been found quite longer than that of the hydrated ion exchange polymer membrane.

© 2004 Elsevier B.V. All rights reserved.

Keywords: Selemion; Bending; Actuator; Hydrated; Dehydrated

1. Introduction

Producing a practical polymer actuator is a significant theme in the engineering field. For instance, one of ion exchange polymer membranes known as Nafion (Dupont) by the commercial name sandwiched between two thin metal layers exhibits a large bending upon a small applied voltage such as 1 V in the hydrated state, where Nafion contains the fixed anions and the free cations in the hydrated state [1–11]. Besides such a low consumption energy and a large deformation, its matrix is so soft and bending motion is quite supple, which must be quite beneficial for the purpose of making, for instance, a robot hand imitating a human hand motion. On the other hand, the conventional actuators such as a shape memory alloy and a piezoelectric, both of which consist of hard matrices, exhibit sometimes undesired too much straightforward motion. Therefore, polymer actuator

will have a significant contribution to the industrial field and our actual life.

As described above, Nafion in the hydrated state exhibits a large bending upon a small applied voltage. It is a quite promising phenomenon, which could lead to the realization of a practical bending mode Nafion actuator. However, there are some problematic issues long hobbling the progress of this kind of polymer actuator researches. Such problems are listed as follows: (i) uncontrollability of the Nafion bending direction by the polarity control of applied voltage after its short use; (ii) large deviation of Nafion bending curvature from the desired curvature after its short use; (iii) the occurrence of bending relaxation; (iv) the short longevity.

One of the ion exchange membranes called Selemion (Asahi Glass Co., Ltd., Japan) sandwiched between two thin metal layers like Nafion, which contains the fixed anions and free cations in the hydrated state, also exhibits the bending upon an applied voltage. But it also has the same problematic issues as Nafion has – (i)–(iv) – in case we use it as a bending mode actuator material. Namely, regardless of ion exchange

* Corresponding author. Tel.: +81 58 293 2492/230 1111.

E-mail address: tmgwhrhs@cc.gifu-u.ac.jp (H. Tamagawa).

polymer membranes type, their bending mechanism must be the same and inevitably the same problems are accompanied for the realization of polymer actuator. Recently, the authors of this paper and our collaborator observed the relatively effective bending of dehydrated Selemion. Although it has been widely believed that the hydration has a requisite role for the induction bending of ion exchange polymer membrane under the applied voltage, it turned out, in fact, to be absolutely possible to induce the bending of dehydrated Selemion. Although the degree of its bending curvature is smaller than the hydrated one, still it is a visibly large enough. Our detailed investigation has revealed that the dehydration treatment on Selemion well overcomes the problematic issues (i)–(iv) described earlier, and it must be true for the other type of ion exchange polymer membranes. We report the detail on it in this paper.

2. Bending of ion exchange polymer membranes

First of all, the widely accepted bending mechanism of hydrated ion exchange membrane is explained.

2.1. Structure of a deformable ion exchange polymer membrane

As an example, we take up Nafion. Nafion is a sheet type polymer with the thickness of around 180 μm . Fig. 1 shows the molecular structure of Nafion. A large number of $-\text{SO}_3\text{H}$ groups are attached to the randomly folding fluorocarbon chains. Fig. 2 shows the Nafion sandwiched between two thin metal layers and it contains a large number of $-\text{SO}_3\text{H}$ functional groups. Both surfaces are metal plated and its matrix is hydrated.

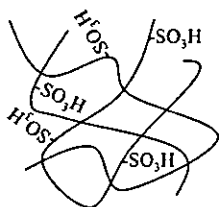


Fig. 1. Molecular structure of Nafion. Main chains consist of fluorocarbon chain and $-\text{SO}_3\text{H}$ functional atomic groups are fixed as branches.

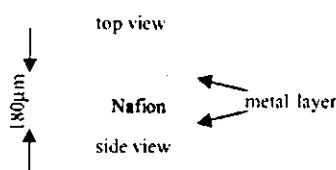


Fig. 2. The structure of Nafion sandwiched between two thin metal layers.

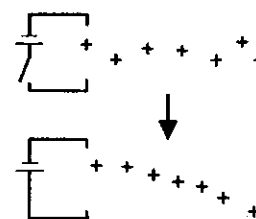


Fig. 3. Bending mechanism of Nafion. The shift of hydrated mobile cations toward the top surface direction by the applied electric field results in the gradient of swelling ratio of Nafion along its thickness direction, and it causes the downward bending of Nafion.

2.2. Bending mechanism

Application of voltage to Nafion causes its bending. It has been widely believed that the hydrated mobile cations contained in Nafion are dragged toward the top surface side of Nafion by the applied voltage – the top surface of Nafion is connected to the negative terminal of power supply – as depicted in Fig. 3, and it causes the gradient of swelling ratio of Nafion in its thickness direction, then consequently, the bending is induced (see Fig. 3 again). It could be speculated that this bending mechanism is not only true for Nafion bending but also true for other type of ion exchange polymer membranes bending as long as they contain the mobile ions in their hydrated state. For example, one of ion exchange membranes called Selemion in the hydrated state can be bent upon an applied voltage [7], where there are two type of Selemions that one is a cation exchange polymer membrane and the other one is an anion exchange polymer membrane, and we have confirmed the induction of both of their bending.

3. Experimental

3.1. Materials

Selemion was employed as a starting material of a specimen. There are two types of Selemion as described above. We took up a Selemion of cation exchange type. The functional atomic group contained in this Selemion is $-\text{SO}_3\text{H}$ and it dissociates into $-\text{SO}_3^-$ and H^+ in the hydrated state. For the purpose of comparing the properties of Selemion with those of Nafion which has been long studied in order to produce a bending mode polymer actuator, Nafion was also employed for this study. Nafion contains $-\text{SO}_3\text{H}$ functional atomic groups, and they dissociate into $-\text{SO}_3^-$ and H^+ in the hydrated state.

3.2. Specimen preparation

Surfaces of Selemion were roughened with a sandpaper. They were plated with silver through the silver mirror reaction [8–10]. They were cut into strips with the dimension

of 20 mm-length \times 2 mm-width. Some of them were stored in a 1 M HCl solution. This process imports the free ions, H^+ and Cl^- , into the Selemion body, and hereafter called hydrated-Selemion (H-S). The rest of them was stored in the desiccator for weeks so as to fully dehydrate, and hereafter called dehydrated-Selemion (D-S).

Nafion was also treated in the same way and cut into the same size of strips, and some of them stored in a 1 M HCl solution was designated as hydrated-Nafion (H-N), and the rest of them dehydrated and stored in the dessicator was designated dehydrated-Nafion (D-N).

3.3. Bending and controllability testing

Bending testing on all four types of specimens, H-S, D-S, H-N and D-S, was performed. Constant voltage was imposed on them, and their tip displacement was measured with a laser displacement meter as a function of time. From the tip displacement data, the specimen curvature was calculated as a function of time. Controllability of bending direction and curvature of these specimens are quite important factors for the purpose of producing polymer actuators. Therefore, we studied these factors through the investigation on the correlation between the bending direction and curvature of specimens and the polarity of applied voltage.

3.4. Oscillation testing

As described above, we had performed the bending testing on all four specimens already, yet it was performed under the condition of constant applied voltage. For the actuator use of ion exchange polymer membrane, it should behave (bend) in perfect agreement with the applied voltage that changes its voltage and polarity for long while. Therefore, oscillation testing was performed on all four types of specimens. Their bending curvature was measured as a function of time upon a sine curve type applied voltage.

4. Results and discussion

4.1. Bending and controllability testing

Fig. 4 shows the time dependence of H-N and H-S upon a constant applied voltage, 1 and 3 V. In this measurement, a strip of specimen with the size of 20 mm-length \times 2 mm-width was fixed horizontally and connected to the power supply as depicted in Fig. 3. The bending curvature of specimen in a downward bending state is defined as a positive curvature, while that of in the upward bending state is defined as a negative curvature. At the initial stage, the higher applied voltage, 3 V, causes the larger bending for both specimens, but such a large bending curvature eventually relaxes with time. The bending relaxation must be caused by the flow of water molecules contained in the specimen toward its bottom surface side. The lower applied voltage, 1 V, appears to sustain a fairly constant curvature of them. Here, we add some

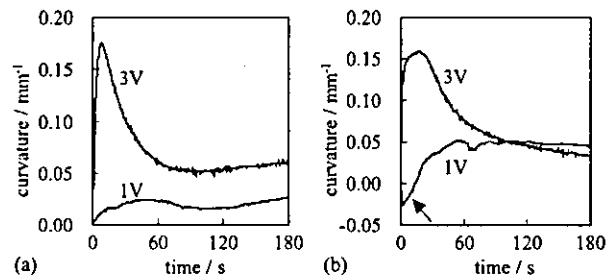


Fig. 4. Time dependence of bending curvature of (a) H-N and (b) H-S upon constant applied voltage, 1 and 3 V.

comment on the bending curvature behavior of H-S upon 1 V applied voltage. Right after the impose of 1 V on H-S, it exhibits upward bending as indicated by an arrow in Fig. 4(b). Although we have yet to identify the cause of it, we strongly speculate that the shift of hydrated anion (primarily hydrated Cl^- in this case) toward the bottom side of H-S induced the upward bending at the initial stage of bending – the bottom surface of H-S is connected to the positive terminal of power supply – as long as the conventionally accepted concept on the cause of bending described in Section 2.2 is right.

Next, we imposed the constant applied voltage on H-N and H-S but changed the voltage polarity periodically. Fig. 5 shows the results. At the moment indicated by arrows, the polarity change was given, where the absolute value of applied voltage had not been changed. None of specimens bending direction were well controlled by the polarity change. None of their bending curvatures were well controlled, either, and all of their curvature values decayed with time. Especially in case the applied voltage is 3 V, neither H-N nor H-S could recover their curvature to the positive side from the negative side after only first polarity change. It must be caused by the destruction of their matrices by the electrolysis of water contained in them. A 3 V applied voltage is so high enough to inevitably cause the vehement electrolysis of water.

Now the same measurements described so far is performed on D-N and D-S (no polarity change). D-N did not exhibit bending upon 1 nor 3 V constant applied voltage. D-S did not exhibit bending upon 1 V constant applied voltage (no

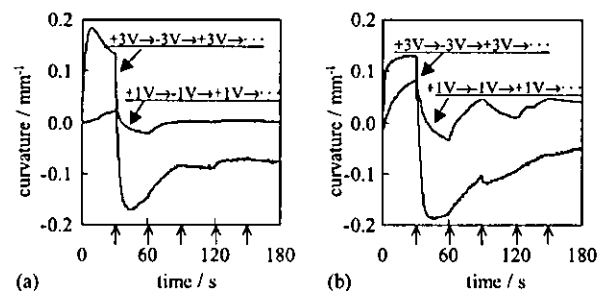


Fig. 5. Time dependence of bending curvature of (a) H-N and (b) H-S upon applied voltage with polarity change but whose absolute values are maintained at 1 and 3 V, namely, $+1\text{ V} \rightarrow -1\text{ V} \rightarrow +1\text{ V} \rightarrow \dots$ and $+3\text{ V} \rightarrow -3\text{ V} \rightarrow +3\text{ V} \rightarrow \dots$. Polarity change of applied voltage is given at the moments indicated by the arrows on the x-axis.

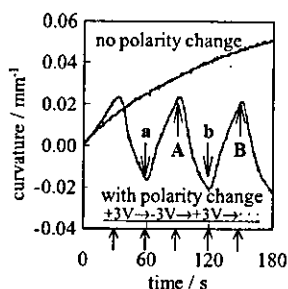


Fig. 6. Time dependence of bending curvature of D-S upon the constant (no polarity change) 3 V applied voltage and upon the 3 V applied voltage with polarity change but whose absolute value is maintained at 3 V where the polarity change is given at the moments indicated by the arrows on the x-axis.

polarity change), either, but it exhibited at 3 V constant applied voltage (no polarity change) as in Fig. 6. Although its curvature is smaller than the hydrated specimen H-S, no bending relaxation was accompanied. It is quite preferable for the actuator. Furthermore, D-S bending curvature perfectly follows the polarity change and the curvature value does not decay with time at all as also shown in Fig. 6. Furthermore, the value of bending curvature of D-S is well controlled by the duration time of applied voltage. For instance, the curvature indicated by the arrow-A in Fig. 6 is realized 30 s after the polarity change indicated by the arrow-a, and the bending curvature indicated by the arrow-B which is the same as that indicated by the arrow-A is also realized 30 s after the polarity change indicated by the arrow-b.

The similar excellent performance was in fact observed about D-N in case the higher voltage of 5 V was applied. But as intuitively understood, the lower consumption energy is better for its practical use. Therefore, we did not perform the further investigation on D-N, but only the observed time dependence of D-N bending curvature upon 5 V constant applied voltage is shown in Fig. 7. The bending is actually observed and no bending relaxation is observed unlike the hydrated Nafion, H-N. The reason of the higher voltage requirement for the D-N bending induction must lie in the thicker matrix of D-N than D-S. The thicker the specimen thickness, d , becomes, the lower the applied electric field, E , becomes, because E is given by $E = V/d$, where V is an applied voltage. The lower E hardly induces the thicker ion exchange polymer membrane bending.

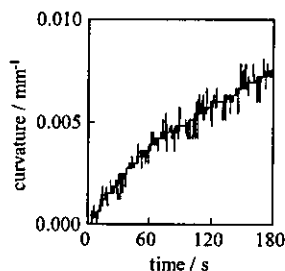


Fig. 7. Time dependence of bending curvature of D-N upon a constant applied voltage, 5 V.

Judging from the widely accepted bending mechanism described earlier, the creation of mobile hydrated ions through the hydration of ion exchange polymer membrane is requisite for the induction of bending. However, our research results suggest that the hydration is not in need for the induction of bending and no hydration bring us even better bending performance of ion exchange polymer membrane. No hydration eliminates the bending relaxation and the poor controllability of bending.

Now it is necessary to elucidate what causes the bending of D-S. Through the observation of D-S bending, we observed the color change of D-S surfaces. Always the surface connected to the negative terminal of power supply becomes white color, while the other surface connected to the positive terminal loses white color, and even through the repetitive polarity change, the surface connected to the negative terminal becomes always white and the other surface connected to the positive terminal always loses its white color accordingly. We measured the surface electric conductivity of D-S and found the high electric conductivity of the white colored surface and the fading of electric conductivity of the non-white colored surface. So this observation suggests that the white color originates from the color of silver, and the shift of silver layer from one surface to the other surface actually occurs in accordance with the change of polarity of power supply. We can strongly speculate that the shift of silver layer plays a critical role for the induction of D-S bending, but we have yet to find out the exact mechanism how it causes the bending. Someone may raise a question that a minute quantity of water remaining in D-S must contribute the creation of hydrated mobile ions in D-S and consequently results in its bending. However, we did not observe any gas bubbles generation from D-S body under 3 V of the applied voltage, when D-S is submerged in a silicone oil, where 3 V is high enough to cause the electrolysis of water generating H_2 and O_2 gases. Further, we did the following experiment. D-S used for a long while under 3 V loses its bending ability. Although we have not identified the cause of bending ability loss, actually D-S loses its bending ability after long use. Since D-S was always used under 3 V for long while, we speculated that no water molecules remained in D-S body because of the water electrolysis. Dotite (Fujikura Kasei Co., Ltd., Tokyo) which is a mixture of silver powder and an adhesive polymer was spread on this long used D-S surfaces, then its bending ability was resurrected. Dotite does not contain any water molecules, therefore the bending of D-S is not caused by the existence of minute quantity of water molecules in it. Namely, the supplied silver on D-S surfaces from Dotite must have played some critical role for the induction of D-S bending. Therefore, silver has some essential role for the induction of bending.

4.2. Oscillation testing

Actuators should have a long and precise controllability for their practical use. In order to see if D-S has such a performance, the alternate voltage of sine curve, whose voltage

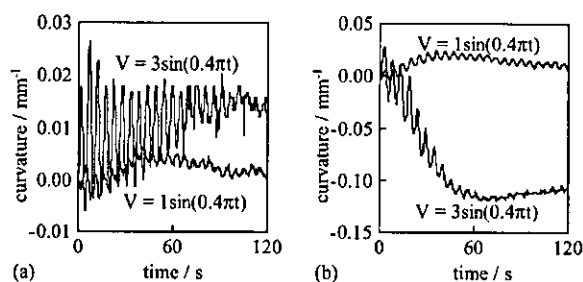


Fig. 8. Time dependence of bending curvature of (a) H–N and (b) H–S upon the alternate applied voltages, $V(V) = 1 \sin(0.4\pi t)$ and $3 \sin(0.4\pi t)$, where t is the time.

is, namely, always changing, was imposed on it, and the time dependence of its curvature was measured. For comparison, the same measurements were performed about H–N and H–S, too. Fig. 8 shows the time dependence of H–N and H–S curvatures upon the alternate applied voltages $V(V) = 1 \sin(0.4\pi t)$ and $3 \sin(0.4\pi t)$, where t is the time. All of them exhibit the oscillation of bending curvature in accordance with the frequency of applied voltage, 0.2 Hz. However, none of them sustains the same amplitude of bending curvature, actually they decay with time, while the amplitudes of applied voltages are maintained constant through the course of this experiment. And none of the center of oscillation of bending curvature is maintained constant at 0 mm^{-1} . They always largely deviate from 0 mm^{-1} , although the center of alternate applied voltage is maintained at 0 mV. On the other hand, the bending curvature amplitude of D–S upon the applied voltage, $V(V) = 3 \sin(0.4\pi t)$, is maintained almost constant, and the center of oscillation of bending curvature is maintained constant at 0 mm^{-1} as shown in Fig. 9. Someone may say that the bending curvature of D–S is so small compared with those of H–N and H–S in Fig. 8 and the center of oscillation of H–N and H–S bending curvature upon $V(V) = 1 \sin(0.4\pi t)$ is fairly close to 0 mm^{-1} . However, the bending curvature of D–S is still large enough so that we can detect it with our naked eyes and the bending curvature of H–N and H–S eventually diminishes toward 0 mm^{-1} after a while unlike that of D–S, and the deviation of the center of oscillation of bending curvature of H–N and H–S is quite large compared with that of D–S which is almost 0 mm^{-1} at any time. The regular oscillation of D–S bending curvature is sustained even at $t = 600 \text{ s}$ (the result is not shown, since it is hard to see

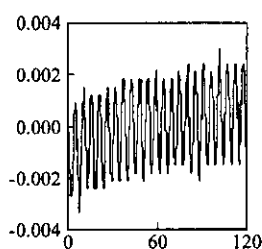


Fig. 9. Time dependence of bending curvature of D–S upon the alternate applied voltage, $V(V) = 3 \sin(0.4\pi t)$.

the detail of bending curvature oscillation from the look of small size diagram). We add that it is true for the dehydrated Nafion, too, although a relatively high applied voltage is in need compared with D–S case. Therefore, besides such excellent bending properties of dehydrated ion exchange polymer membranes, they can acquire quite long longevity of bending performance through the dehydration treatment. If the bending is primarily caused by the shift of hydrated mobile ions, such an excellent and long sustainable bending behavior cannot be realized, since water molecules are easily decomposed into H_2 and O_2 through the electrolysis. Dehydration can let the ion exchange membranes exhibit the better performance, when they are used as the bending mode actuator materials.

5. Conclusion

Dehydration of Selemion was found to be an efficient method resulting in the precisely controllable bending of it with a longer longevity. The same was true for Nafion, too, and it let us speculate that any dehydrated ion exchange polymer membranes can be bent precisely at our will for a long period. Dehydration could become a new principle to realize a practical ion exchange polymer membrane actuator.

Acknowledgments

We would like to express our gratitude to Nihon Polymer (Aichi, Japan) and Asahi Glass Co., Ltd. (Tokyo, Japan) for their kind service to purchase Nafion and Selemion. This research was financially supported by Health and Labour Science Research Grants of Research on Advanced Medical Technology (No. H14-nano-021) from Ministry of Health Labour and Welfare, The Mikiya Science and Technology Foundation, and Izumi Science and Technology Foundation, all Japan.

References

- [1] K. Oguro, Y. Kawami, H. Takenaka, Bending of an ion-conducting polymer film-electrode composite by an electric stimulus at low voltage, *Trans. J. Micromach. Soc.* 5 (1992) 27.
- [2] K. Asaka, K. Oguro, Y. Nishimura, M. Mizuhara, H. Takenaka, Bending of polyelectrolyte membrane-platinum composites by electric stimuli I, response characteristics to various waveforms, *Polym. J.* 27 (1995) 436.
- [3] K. Salehpoor, M. Shahinpoor, M. Mojarad, Actuators made from ion-exchange membrane-metal composites, smart materials technologies, *Proc. SPIE Smart Mater. Struct. San Diego* 3040 (1997) 192.
- [4] M. Shahinpoor, M. Mojarad, K. Salehpoor, Electrically induced large amplitude vibration and resonance characteristics of ionic polymeric membrane-metal composites artificial muscles, *Proc. SPIE Smart Mater. Struct. San Diego* 3041 (1997) 829.
- [5] Y. Bar-Cohen, T. Xue, M. Shahinpoor, K. Salehpoor, J. Simpson, J. Smith, Low-mass muscle actuators using electroactive polymers (EAP), *Proc. SPIE Smart Mater. Struct. San Diego* 3324 (1998) 218.

- [6] M. Uchida, M. Taya, Solid polymer electrolyte actuator using electrode reaction, *Polymer* 42 (2001) 9281.
- [7] T. Nakagawa, Y. Takase, A. Abe, T. Watanabe, H. Tamagawa, F. Nogata, The bending characteristics of IPMCs containing fixed negative or positive charges under an electric field, *JSME Conference preprint*, Nagoya, Japan, 2003, p. 67.
- [8] H. Tamagawa, F. Nogata, T. Watanabe, A. Abe, K. Yagasaki, Bending curvature and generated force by Nafion actuator, *IEEE ICIT'02*, Bangkok, 2002, p. 945.
- [9] H. Tamagawa, F. Noagata, T. Watanabe, A. Abe, K. Yagasaki, J.-Y. Jin, Influence of metal plating treatment on the electric response of Nafion, *J. Mater. Sci.* 38 (2003) 1039.
- [10] H. Tamagawa, K. Yagasaki, F. Nogata, Mechanical characteristics of ionic polymer–metal composite in the process of self-bending, *J. Appl. Phys.* 92 (2002) 7614.
- [11] S. Popovic, Design of electro-active polymer gels as actuator materials, PhD Thesis, University of Washington, 2001.

Improved controllability of a fully dehydrated Selemion actuator

Hirohisa Tamagawa, and Fumio Nogata

Department of Human and Information Systems, Faculty of Engineering, Gifu University, Gifu, Japan
(Tel : +81-58-293-2492; E-mail: tmgwhrhs@cc.gifu-u.ac.jp)

Abstract: Ion exchange polymer membrane in the dehydrated state was found to exhibit bending upon a small applied voltage, although the investigations on the hydrated ion exchange polymer membrane bending behavior have been performed quite intensively for more than a decade for the purpose of producing a practical polymer actuator. Our investigation on the dehydrated ion exchange polymer membrane has revealed that its bending direction is perfectly controllable by the polarity control of applied voltage and the degree of its bending curvature is also almost completely determined by the control of duration time of voltage application on it, while the hydrated ion exchange polymer membranes lack of such properties. Furthermore the longevity of dehydrated ion exchange polymer membrane sustaining such a highly controllable properties has been found quite longer than that of the hydrated ion exchange polymer membrane.

Keywords: Selemion, bending, actuator, hydrated, dehydrated

1. INTRODUCTION

One of ion exchange polymer membranes known as Nafion (Dupont) by the commercial name sandwiched between two thin metal layers exhibits a large bending upon a small applied voltage such as 1V in the hydrated state, where Nafion contains the fixed anions, $-SO_3^-$, and the free cations, H^+ , in the hydrated state [1-11]. Besides such a low consumption energy and a large bending, its matrix is so soft and bending motion is quite supple, which must be quite beneficial for the purpose of making, for instance, a robot imitating a human like soft motion. Therefore polymer actuator will have a significant contribution to the industrial field and our actual life.

As described above, Nafion in the hydrated state exhibits a large bending upon a small applied voltage, which could lead to the realization of a practical bending mode Nafion actuator. However, there are some problematic issues long hobbling the progress of this kind of polymer actuator researches. Such problems are listed as follows: i) uncontrollability of the Nafion bending direction by the polarity control of applied voltage after its short use, ii) the large deviation of Nafion bending curvature from the desired curvature after its short use, iii) the occurrence of bending relaxation, iv) the short longevity.

One of the ion exchange membranes called Selemion (Asahi Glass Co., Ltd. Japan) (there are two types of Selemion, one is a cation exchange type and another one is an anion exchange type, and here the former one is mainly focused on) sandwiched between two thin metal layers just like Nafion, which contains the fixed anions, $-SO_3^-$, and free hydrated cations, H^+ , in the hydrated state, also exhibits the bending upon an applied voltage. But it also has the same problematic issues as Nafion has – i), ii), iii), and iv) – in case we use it as a bending mode actuator material. Namely, regardless of ion exchange polymer membranes type, their bending mechanism must be the same and inevitably the same problems are accompanied for the realization of polymer actuator. Recently, the authors of this paper and our collaborator observed the relatively effective bending of largely (not fully) dehydrated ion exchange polymer membrane [12]. Although it has been widely believed that the hydration has a requisite role for the induction bending of ion exchange polymer membrane under the applied voltage, it turned out, in fact, to be absolutely possible to induce the bending of largely dehydrated ion exchange polymer membrane. Although the degree of its bending curvature is

smaller than the hydrated one, still it is a visibly large enough. Our detailed investigation has revealed that the dehydration treatment on ion exchange polymer membrane well overcomes the problematic issues i), ii), iii) and iv).

2. BENDING OF ION EXCHANGE POLYMER MEMBRANE

First of all, the widely accepted bending mechanism of hydrated ion exchange membrane is explained.

2.1. Structure of a bendable ion exchange polymer membrane

As an example, we take up Nafion. Nafion is a sheet type polymer with the thickness of around 180 μ m. Fig.1 shows the molecular structure of Nafion. A large number of $-SO_3H$ groups are attached to the randomly folding fluorocarbon chains. Fig. 2 is the Nafion sandwiched between two thin metal layers and it contains a large number of $-SO_3H$ functional groups. Both surfaces are metal plated and its matrix is hydrated.

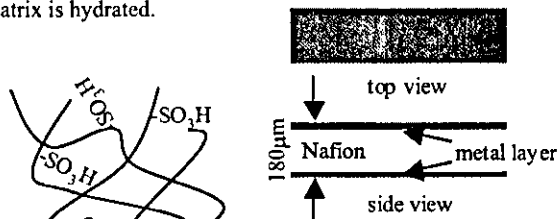


Fig. 1 Structure of Nafion Main chains are fluorocarbon

Fig. 2 The structure of Nafion sandwiched between two thin metal layers

2.2. Bending mechanism

Application of voltage to Nafion causes its bending. It has been widely believed that the hydrated mobile cations contained in Nafion are dragged toward the top surface side of Nafion by the applied voltage – the top surface of Nafion is connected to the negative terminal of power supply – as depicted in Fig. 3, and it causes the gradient of swelling ratio of Nafion in its thickness direction, then consequently, the bending is induced (see Fig. 3 again).

2.3. Evidences supporting the widely accepted bending mechanism

If the bending mechanism described above is absolutely

right, the ion exchange membrane which contains the free anions and the fixed cations must exhibit the bending in the direction opposite to the bending direction of Nafion, since the hydrated mobile anions contained in that ion exchange polymer membrane is expected to be dragged toward its surface connected to the positive terminal of power supply, then it must consequently cause the bending in the opposite direction as depicted in Fig. 4. Indeed, Nakagawa et al. observed such a phenomenon between the cation exchange type Nafion and the anion exchange type Selemion [7]. Nakagawa et al. forcibly imported CuSO_4 solution into both Nafion and Selemion bodies. Both Nafion and Selemion come to contain both cations, Cu^{2+} , and anions, SO_4^{2-} . However, the free cations, Cu^{2+} , must outnumber the free anions, SO_4^{2-} , in Nafion, while the free anions, SO_4^{2-} , must outnumber the free cations, Cu^{2+} , in Selemion, because Nafion and Selemion contain the fixed anions and cations, respectively, and electroneutrality should be valid in their bodies. Therefore it is expected that Nafion bending is dominated by the hydrated free Cu^{2+} primarily and Selemion bending is dominated by the hydrated free SO_4^{2-} primarily. Thus the bending mechanism described in the section 2.2. predicts that the downward bending of Nafion and upward bending of Selemion. Fig. 5 shows the curvature of Nafion and Selemion, where the bending curvature of Nafion is defined as positive. Since Selemion's curvature in Fig. 5 is negative, Nafion and Selemion exhibit bending in the opposite direction each other as predicted.

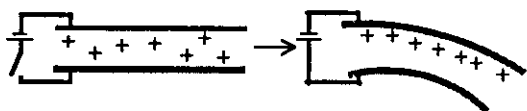


Fig. 3 Bending mechanism of Nafion The shift of hydrated mobile cations toward the top surface direction by the applied electric field results in the gradient of swelling ratio of Nafion along its thickness direction, and it causes the downward bending of Nafion



Fig. 4 Bending of the ion exchange polymer membrane caused by the shift of hydrated free anions

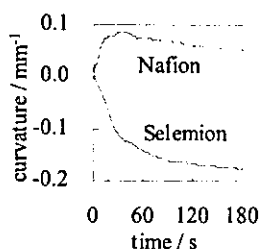


Fig. 5 Time dependence of the curvature of a cation exchange type Nafion and a anion exchange type Selemion swollen with CuSO_4 solution upon 1V

3. EXPERIMENTAL

3.1. Materials

A cation exchange type Selemion was employed as a starting material of a specimen. The functional atomic group contained in this Selemion is $-\text{SO}_3\text{H}$ and it dissociates into $-\text{SO}_3^-$ and H^+ in the hydrated state. For the purpose of comparing the properties of Selemion with those of Nafion which has been long studied in order to produce a bending mode polymer actuator, Nafion was also employed for this study.

3.2. Specimen preparation

Surfaces of Selemion were roughened with a sandpaper. They were plated with silver through the silver mirror reaction [8-10]. Some silver plated Selemions were stored in a 1M HCl solution. This process imports the free ions, H^+ and Cl^- , into the Selemion body, and hereafter called H-S (Hydrated-Selemion). The rest of it was stored in the desiccator for weeks so as to fully dehydrate, and hereafter called D-S (Dehydrated-Selemion).

Nafion was also treated in the same way, and some of it stored in a 1M HCl solution was designated as H-N (Hydrated-Nafion), and the rest of it dehydrated and stored in the dessicator was designated D-N (Dehydrated-Nafion).

3.3. Bending and controllability testing

Bending testing on all four types of specimens, H-S, D-S, H-N and D-S, was performed. Constant voltage was imposed on them, and their tip displacement was measured with a laser displacement meter as a function of time. Tip displacement data was converted into the curvature through the simple calculated. Controllability of bending direction and curvature of these specimens are quite important factors for the practical polymer actuators. Therefore we studied these factors through the investigation on the correlation between the bending direction & curvature of specimens and the polarity of applied voltage.

3.4. Oscillation testing

As described above, we had performed the bending testing on all four specimens already, yet it was performed under the constant applied voltage. For the actuator use of ion exchange polymer membrane, it should behave (bend) in perfect agreement with the applied voltage that changes its voltage and polarity for long while. Therefore oscillation testing was performed on all four types of specimens. Their bending curvature was measured as a function of time upon a sine curve type applied voltage.

4. RESULTS AND DISCUSSION

4.1. Bending and controllability testing

Fig. 6 shows the time dependence of H-N and H-S upon a constant applied voltage, 1 and 3V. In this measurement, a strip of specimen with the size of 20mm-length \times 2mm-width was fixed horizontally and connected to the power supply as depicted in Fig. 3. The bending curvature of specimen in the a downward bending state is defined as a positive curvature, while that of in the upward bending state is defined as a negative curvature. At the initial stage, the higher applied voltage, 3V, causes the larger bending for both specimens, but such a large bending curvature eventually relaxes with time.

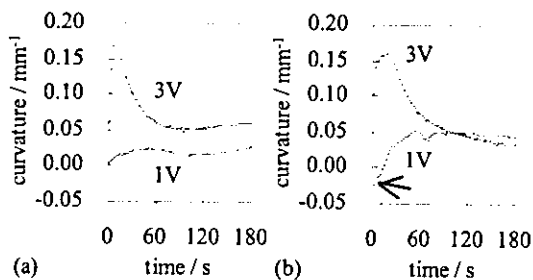


Fig. 6 Time dependence of bending curvature of (a) H-N and (b) H-S upon constant applied voltage, 1 and 3V

The lower applied voltage, 1V, appears to sustain a fairly constant curvature of them for long while after around $t = 30$ (s). Here we add some comment on the bending curvature behavior of H-S upon 1V applied voltage. Right after the impose of 1V on H-S, it exhibits upward bending as indicated by an arrow in Fig. 6(b). Although we have yet to identify the cause of it, we strongly speculate that the shift of hydrated anion (primarily hydrated Cl⁻ in this case) toward the bottom side of H-S induced the upward bending at the initial stage of bending – the bottom surface of H-S is connected to the positive terminal of power supply –, as long as the conventionally accepted concept on the cause of bending described in the section 2.2 is right.

Next we imposed the voltage, V, regularly changing its polarity – $V = +1V \rightarrow -1V \rightarrow +1V \rightarrow \dots, +3V \rightarrow -3V \rightarrow +3V \rightarrow \dots$ – on H-N and H-S. Fig. 7 shows the results. At the moments indicated by the arrows on the x-axis, the polarity change was given. None of specimens bending direction were well controlled by the polarity change. None of their bending curvatures were well controlled, either, and all of their curvature values decayed with time. Especially in case the applied voltage is the alternation of +3V and -3V, neither H-N nor H-S could recover their curvature to the positive side from the negative side after the first polarity change. It must be caused by the destruction of their matrices by the electrolysis of water contained in them. The applied voltages of 3V as absolute value is so high enough to inevitably cause the vehement electrolysis of water.

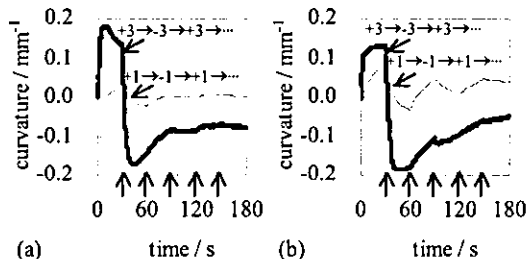


Fig. 7 Time dependence of bending curvature of (a) H-N and (b) H-S upon 1 and 3V regularly changing their polarity, namely, $+1V \rightarrow -1V \rightarrow +1V \rightarrow \dots$ and $+3V \rightarrow -3V \rightarrow +3V \rightarrow \dots$. Polarity change of applied voltage is given at the moments indicated by the arrows on the x-axis.

Now the same measurements described so far is performed on D-N and D-S. D-N did not exhibit bending upon 1 nor 3V constant applied voltage (no polarity change). D-S did not exhibit bending upon 1V constant applied voltage (no polarity change), either, but it exhibited at 3V constant applied voltage (no polarity change) as in Fig. 8. Although its curvature is smaller than the hydrated specimen H-S, we observed a good property that no bending relaxation was accompanied. It is quite preferable for the actuator. Furthermore D-S bending curvature perfectly follows the polarity change and the curvature value does not decay with time at all as also shown in Fig. 8. Furthermore, the value of bending curvature of D-S is well controlled by the duration time of applied voltage. For instance, the curvature indicated by the arrow-A in Fig. 8 is realized 30 seconds after the polarity change indicated by the arrow-a, and the bending curvature value indicated by the arrow-B which is the same as that indicated by the arrow-A is also realized 30 seconds after the polarity change indicated by the arrow-b.

The similar excellent performance was in fact observed about D-N in case the higher voltage of 5V (no polarity

change) was applied. But as intuitively understood, the lower consumption energy is better for its practical use. Therefore we did not perform the further investigation on D-N, but only the observed time dependence of D-N bending curvature upon 5V constant applied voltage is shown in Fig. 9. The bending is actually observed and no bending relaxation is observed unlike the hydrated Nafion, H-N. The reason of the higher voltage requirement for the D-N bending induction must lie in the thicker matrix of D-N than D-S. The thicker the specimen thickness, d , becomes, the lower the applied electric field, E , becomes, because E is given by $E = V/d$, where V is an applied voltage. The lower E hardly induces the thicker ion exchange polymer membrane bending.

Judging from the widely accepted bending mechanism described earlier, the creation of mobile hydrated ions through the hydration of ion exchange polymer membrane is requisite for the induction of bending. However, our research results suggest that the hydration is not in need for the induction of bending and no hydration bring us even better bending performance of ion exchange polymer membrane. No hydration eliminates the bending relaxation and the poor controllability of bending.

Now it is necessary to elucidate what causes the bending of D-S. Through the observation of D-S bending, we observed the color change of D-S surfaces. Always the surface connected to the negative terminal of power supply becomes white color, while the other surface connected to the positive terminal loses white color, and even through the repetitive polarity change, the surface connected to the negative terminal becomes always white and the other surface connected to the positive terminal always loses its white color accordingly. We measured the surface electric conductivity of D-S and found the high electric conductivity of the white colored surface and the fading of electric conductivity of the non-white colored surface. So this observation suggests that the white color originates from the color of silver, and the shift of silver layer from one surface to the other surface actually occurs in accordance with the change of polarity of power supply. We can strongly speculate that the shift of silver layer plays a critical role for the induction of D-S bending, but we have yet to find out the exact mechanism how it causes the bending. Someone may raise a question that a minute quantity of water remaining in D-S must contribute the creation of hydrated mobile ions in D-S and consequently

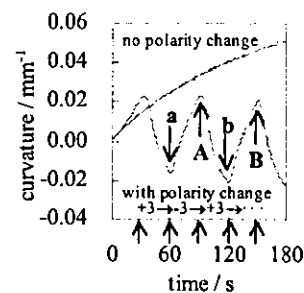


Fig. 8 Time dependence of bending curvature of D-S upon the constant (no polarity change) 3V applied voltage and upon 3V applied voltage regularly changing their polarity, namely, $+3V \rightarrow -3V \rightarrow +3V \rightarrow \dots$. Polarity change is given at the moments indicated by the arrows on the x-axis.

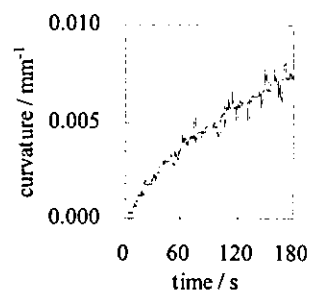


Fig. 9 Time dependence of bending curvature of D-N upon a constant applied voltage, 5V

results in its bending. However, we did not observe any gas bubbles generation from D-S body under 3V of the applied voltage, when D-S is submerged in a silicone oil, where 3V is high enough to cause the electrolysis of water generating H₂ and O₂ gases. Further, we did the following experiment. D-S used for a long while under 3V loses its bending ability. Although we have not identified the cause of bending ability loss, actually D-S loses its bending ability after long use. Since D-S was always used under 3V for long while, we speculated that no water molecules remained in D-S body because of the water electrolysis. Dotite (Fujikura Kasei Co., Ltd, Tokyo) which is a mixture of silver powder and an adhesive polymer was spread on this long used D-S surfaces, then its bending ability was resurrected. Dotite does not contain any water molecules, therefore the bending of D-S is not caused by the existence of minute quantity of water molecules in it. Namely, the supplied silver on D-S surfaces from Dotite must have played some role for the induction of D-S bending. Therefore silver must have some essential role for the induction of bending.

4.2. Oscillation testing

Actuators should have a long and precise controllability for their practical use. In order to see if D-S has such a performance, the alternate voltage of sine curve, whose voltage is, namely, always changing, was imposed on it, and the time dependence of its curvature was measured. For comparison, the same measurements were performed about H-N and H-S, too. Fig. 10 shows the time dependence of the curvature of H-N and H-S upon the alternate applied voltages, $V = 1\sin(0.4\pi t)$ (volt) and $3\sin(0.4\pi t)$ (volt), where t is time. Both of them exhibit the oscillation of bending curvature in accordance with the frequency of applied voltage, 0.2 (Hz). However, none of them sustains the same amplitude of bending curvature even for short while. Actually they decay with time soon after the onset of voltage application, while the amplitudes of applied voltages are maintained constant through the course of this experiment. And none of the center of oscillation of bending curvature is maintained constant at 0 (mm^{-1}) even for short while, either. They always largely deviate from 0 (mm^{-1}), although the center of alternate applied voltage is maintained at 0 (mV). On the other hand, the bending curvature amplitude of D-S upon the applied voltage, $V = 3\sin(0.4\pi t)$ (volt), is maintained almost constant, and the center of oscillation of bending curvature is maintained constant at 0 (mm^{-1}) for longer while than the others as shown in Fig. 11. Someone may say that the bending curvature of D-S is so small compared with those of H-N and H-S in Fig. 10 and the center of oscillation of H-N and H-S bending curvature upon $V = 1\sin(0.4\pi t)$ (volt) is fairly close to 0 (mm^{-1}). However, the bending curvature of

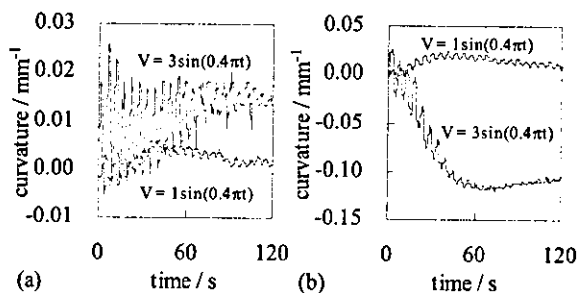


Fig. 10 Time dependence of bending curvature of (a) H-N and (b) H-S upon the alternate applied voltages, $V = 1\sin(0.4\pi t)$ (volt) and $3\sin(0.4\pi t)$ (volt), where t is time.

D-S is still large enough so that we can detect it with our naked eyes and the bending curvature of H-N and H-S eventually diminishes toward 0 (mm^{-1}) after a while unlike that of D-S, and the deviation of the center of oscillation of bending curvature of H-N and H-S is quite large compared with that of D-S which is almost 0 (mm^{-1}) at any time. Though the amplitude of oscillation of H-N and H-S bending

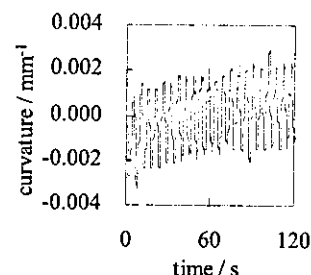


Fig. 11 Time dependence of bending curvature of D-S upon the alternate applied voltage, $V = 3\sin(0.4\pi t)$ (volt)

curvature gradually diminishes toward 0 (mm^{-1}) and the center of their oscillation gradually deviates from 0 (mm^{-1}), the fairly regular oscillation of D-S bending curvature is sustained even up to $t = 3600$ (s) (the result is not shown, since it is hard to see the detail of bending curvature oscillation from the look of small size diagram). We add that it is true for the dehydrated Nafion, too, although a relatively high applied voltage is in need compared with D-S case. Therefore, besides such excellent bending properties of dehydrated ion exchange polymer membranes, they can acquire quite long longevity of bending performance through the dehydration treatment. If the bending is primarily caused by the shift of hydrated mobile ions, such an excellent and long sustainable bending behavior cannot be realized, since water molecules are easily decomposed into H₂ and O₂ through the electrolysis.

Dehydration can let the ion exchange membranes exhibit the better performance, when they are used as the bending mode actuator materials.

5. CONCLUSION

Dehydration of Selemion was found to be an efficient method resulting in the precisely controllable bending of it with a longer longevity. The same was true for Nafion, too, and it let us speculate that any dehydrated ion exchange polymer membranes can be bent precisely at our will for a long period. Dehydration could become a new principle to realize a practical ion exchange polymer membrane actuator.

ACKNOWLEDGMENT

We'd like to express our gratitude to Nihon Polymer (Aichi, Japan) and Asahi Glass Co., Ltd. (Tokyo, Japan) for their kind service to purchase Nafion and Selemion. This research was financially supported by Health and Labour Science Research Grants of Research on Advanced Medical Technology (No. H14-nano-021) from Ministry of Health Labour and Welfare, The Mikiya Science and Technology Foundation, and Izumi Science and Technology Foundation, all Japan.

REFERENCES

- [1] K. Oguro, Y. Kawami and H. Takenaka, "Bending of an Ion-Conducting Polymer Film-Electrode Composite by an Electric Stimulus at Low Voltage," *Trans. J. Micromachine Soc.*, Vol.5, pp. 27-30, 1992.
- [2] K. Asaka, K. Oguro, Y. Nishimura, M. Mizuhara, H. Takenaka, "Bending of Polyelectrolyte Membrane-Platinum Composites by Electric Stimuli I,

- Response Characteristics to Various Waveforms," *Polym. J.*, Vol.27, pp. 436-440, 1995.
- [3] K. Salehpoor, M. Shahinpoor, M. Mojjarrad, "Actuators Made From Ion-Exchange Membrane-Metal Composites, Smart Materials Technologies," *Proc. SPIE Smart Mater. Struct.*, San Diego, Vol.3040, pp. 192-198, 1997.
- [4] M. Shahinpoor, M. Mojjarrad, K. Salehpoor, "Electrically Induced Large Amplitude Vibration and Resonance Characteristics of Ionic Polymeric Membrane-Metal Composites Artificial Muscles," *Proc. SPIE Smart Mater. Struct.*, San Diego, Vol.3041, pp. 829-838, 1997.
- [5] Y. Bar-Cohen, T. Xue, M. Shahinpoor, K. Salehpoor, J. Simpson, J. Smith, "Low-mass muscle actuators using electroactive polymers (EAP)," *Proc. SPIE Smart Mater. Struct.*, San Diego, Vol.3324, pp. 218-223, 1998.
- [6] M. Uchida, M. Taya, "Solid Polymer Electrolyte Actuator using Electrode Reaction," *Polymer*, Vol.42, pp. 9281-9285, 2001.
- [7] T. Nakagawa, Y. Takase, A. Abe, T. Watanabe, H. Tamagawa, F. Nogata, "The bending characteristics of IPMCs containing fixed negative or positive charges under an electric field," *JSME conference preprint*, Nagoya, Japan, pp. 67-68, 2003.
- [8] H. Tamagawa, F. Nogata, T. Watanabe, A. Abe, K. Yagasaki, "Bending curvature and generated force by Nafion actuator," *Proc. IEEE ICIT'02*, Bangkok, pp. 945-949, 2002.
- [9] H. Tamagawa, F. Noagata, T. Watanabe, A. Abe, K. Yagasaki, J.-Y. Jin, "Influence of metal plating treatment on the electric response of Nafion," *J. Mater. Sci.*, Vol.38, pp. 1039-1044, 2003.
- [10] H. Tamagawa, K. Yagasaki, F. Nogata, "Mechanical Characteristics of ionic polymer-metal composite in the process of self-bending," *J. Appl. Phys.*, Vol.92, pp. 7614-7618, 2002.
- [11] S. Popovic, Ph.D thesis, DESIGN OF ELECTRO-ACTIVE POLYMER GELS AS ACUATOR MATERIALS, University of Washington, (2001).
- [12] H. Tamagawa, F. Nogata, S. Popovic, "Bending of largely dehydrated polymer membranes coated with a polymer-metal composite," to be submitted.

原 著

リポソーム中に存在するスピンラベル剤の ESR スペクトルと全身麻酔薬の影響

渋谷真希子¹⁾ 平沖 敏文²⁾ 木村 邦衛¹⁾
堤 耀廣²⁾ 鈴木 邦明³⁾ 福島 和昭¹⁾

抄 録：スピンラベル剤 5-DSA および 16-DSA を組み込んだリポソームにおける電子スピン共鳴 (ESR) スペクトルを指標に全身麻酔薬がスピンラベル剤周囲の環境に与える影響について検討した。

リポソーム構成脂質としてフォスファチジルコリンを用い、多重層リポソーム (MLV) と小さな一枚膜リポソーム (SUV) の 2 種類を作成した。全身麻酔薬として、セボフルレン、イソフルレン、ハロセン、エーテル、エタノール、プロポフォル、サイアミラルを用いた。得られた ESR スペクトルの線形変化をみると同時にオーダーパラメーター S および回転相関時間 τ を計算した。

MLV に 5-DSA をラベルした ESR スペクトルは、SDS 水溶液中のスペクトルに比べラジカルの運動に異方性があり、回転運動の速度が遅いことを示していた。16-DSA でラベルされた標本のスペクトルは 5-DSA に比べ比較的鋭いシャープな 3 本のシグナルを示した。また、5-DSA および 16-DSA をラベルした際の ESR スペクトルの S は両者にて異なり、両ラベル剤のニトロキシドラジカルは二重膜の異なる部分に存在することが示された。スペクトル強度は、セボフルレンやイソフルレンでは麻酔薬の濃度に伴って増大し、またハロセン、エーテル、エタノールでは高濃度を加えたときに増大したものの、いずれの麻酔薬を添加しても膜流動性の指標となる S や τ にはほとんど影響しなかった。さらに、SUV での S と τ をみると MLV におけるパラメーター値との違いはほとんどなく、リポソーム膜の形態による影響はないと考えられた。

以上の結果から、麻酔薬は脂質二重膜の表層にとどまっておき、ニトロキシドラジカルの存在する脂質の深い疎水部や比較的浅い親水部まで麻酔薬は影響を及ぼさないことが示唆された。

キーワード：電子スピン共鳴、リポソーム、全身麻酔薬、オーダーパラメーター S 、回転相関時間 τ

I. 緒 言

電子スピン共鳴 (ESR) を用いるスピンラベル法は、1965年に大西と McConnell¹⁾により考案され、安定なラジカルをもつスピンラベル剤を対象物に化学的に結合させて、そのラジカルの ESR スペクトルから対象物の周囲の環境および運動状態を調べるという方法である。我々は以前の研究において、ESR スペクトルの測定による全身麻酔薬作用機構の解明を目的に、ステアリン酸スピンラベル剤を含む水溶液中のドデシル硫酸ナトリウム (SDS) ミセルを生体膜のモデルとして全身麻酔薬を加え、スピンラベル剤の周囲の環境に与える麻酔薬の影響について検討した結果、以下のことが結果を得た²⁾。

1) アルキル鎖中のラジカルの位置が異なる 2 つのステアリン酸スピンラベル剤 5-doxyl stearic acid (以下 5-DSA) および 16-doxyl stearic acid (以下 16-DSA) (構造式を Fig. 1 に示す) をそれぞれ含む SDS 水溶液の ESR スペクトルより得られた結果は、ラジカルの位置がそれぞれミセルの表層の親水基付近と内部の疎水基付近という異なる場所であることを示していた。したがって、5-DSA と 16-DSA によりそれぞれ膜の表層付近および比較的内部の情報を得ることができる^{3,4)} 生体膜の場合と同様に議論できることが示された。

2) ラベル剤を含む SDS 水溶液に麻酔薬を添加した際の ESR スペクトルのパラメーター変化は、数種の麻酔薬では有意であったが、その変化量は小さかった。また変化の

^{1),3)} 〒060-8586 札幌市北区北13条西7丁目

²⁾ 〒060-8628 札幌市北区北13条西8丁目

¹⁾ 北海道大学大学院歯学研究科口腔病態学講座歯科麻酔学教室 (主任：福島和昭 教授)

²⁾ 北海道大学大学院工学研究科量子物理工学専攻物質物理工学講座分子物理工学 (主任：堤 耀廣 教授)

³⁾ 北海道大学大学院歯学研究科口腔病態学講座細胞分子薬理学教室 (主任：鈴木邦明 教授)

[受付：平成16年4月20日] [受理：平成16年5月21日]

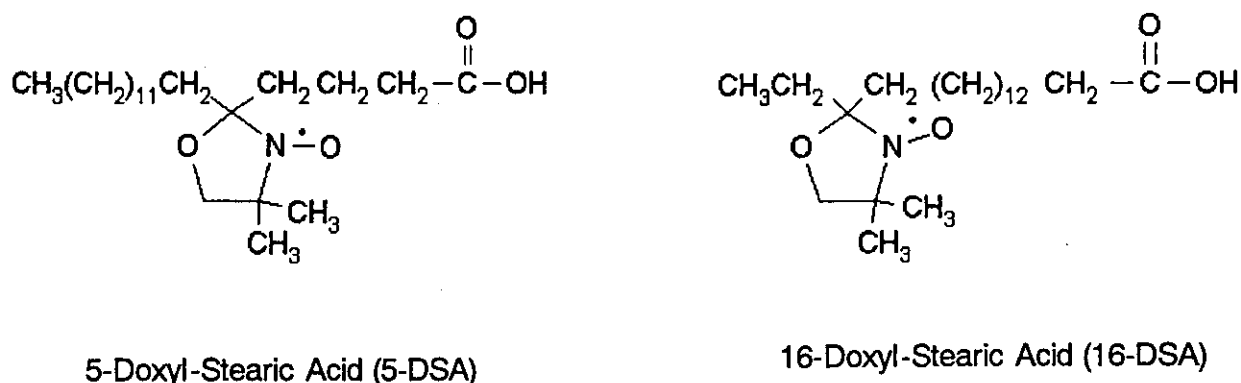


Fig. 1 Structure of 5-DSA and 16-DSA.

度合いは加えた麻酔薬の種類や濃度によって様々であり、麻酔薬の種類により、スピラベル剤周囲の環境変化の度合いが異なることが示唆された。

しかし、SDS は実際に生体内に存在する物質ではない。そこで、次の段階として生体膜構成物質であり、麻酔薬の作用部位として議論されている脂質を用いた検討を試みた。

脂質から構成される二重層構造の閉鎖小胞はリボソームと呼ばれ、作成の容易さから広く生体膜モデルとして使われ有用な情報を提供してきた。リボソームはその形態から、多重層リボソーム (multilamellar vesicle: MLV)、小さな一枚膜リボソーム (small unilamellar vesicle: SUV)、大きな一枚膜リボソーム (large unilamellar vesicle: LUV) に大別される^{5,6)}。MLV は大きさが0.5-10 μm と不均一であるものの、安定性に優れ調整法が最も簡便である。SUV は大きさが100nm 以下で比較的均一であるが安定性は多少問題があるとされる。LUV は0.1-1 μm 程度の直径で内水相に高分子を保持できるため薬物や遺伝子などを内包させて生体内に投与する薬物キャリアーとして期待されている。

生体膜の主要な構成脂質であるフォスファチジルコリン (PC) はその構造の特性から単独で安定したリボソーム構造をとりやすい。そこで今回我々は、5-DSA、16-DSA をそれぞれ含んだ PC リボソームとして MLV および SUV を作成し、ESR スペクトルを測定することによって、SDS ミセルにおけるスペクトルとの相違やリボソームの種類による相違、スピラベル剤周囲の環境に与える麻酔薬の影響、麻酔薬の濃度による変化について検討した。

II. 材料と方法

1. 材料

5-DSA および 16-DSA および PC は Aldrich 社製のものを使用した。セボフルレン、イソフルレンはアポットジャパン社製、ハロセンは武田薬品工業社製、プロポフォルはアストラゼネカ社製、サイアミラルは三菱ウェルファーマ社製、その他の試薬は特級を使用した。

5-DSA および 16-DSA は50mM の濃度になるようにメタノールに溶解し、-40℃にて保存した。

2. 方法

(i) MLV の作成^{5,6)}

卵黄由来の PC をクロロホルムに溶解し、最終濃度が 500 μM となるように 5-DSA または 16-DSA を加えた。次に回転式エバポレーターにて溶媒を除去し、さらにデシケーターに 2 時間以上保管して完全に溶媒を除去した。作成された脂質フィルムに 25mM Tris-HCl (pH 7.4) buffer を加えボルテックスミキサーにて常温でよく攪拌し白濁した MLV 溶液を得た。

(ii) SUV の作成^{5,6)}

MLV を作成した後、プローブ型ソニケーターにて 30 分間溶液が透明になるまで超音波処理した。その後、3000 rpm にて遠心を行い、ソニケーターのプローブから溶出したチタニウムを沈殿させ SUV を得た。

(iii) 測定試料の作成

麻酔薬は、臨床で用いた際に測定された血中濃度と同程度の濃度 (エタノールに関しては酪酐状態となる血中濃度と同程度の濃度) を臨床濃度⁷⁻¹²⁾ (セボフルレンは 350 μM, イソフルレンは 10.5mg/dl, ハロセンは 28.1mg/dl, エーテルは 150mg/dl, エタノールは 0.2%, サイアミラルは 25 μg/ml, プロポフォルは 10mg/ml), とした。麻酔薬を加えた後はただちにキャップをして麻酔薬が揮発するのを防止した。ボルテックスミキサーにて攪拌した後 50 μl をマイクロシリンジにて取り出しガラス製キャピラリー (外径 1.52mm, 内径 1.09mm, 長さ約 8.5cm) に注入し、揮発を防ぐためワックスとパラフィルムによる栓をして測定した。

3. ESR 測定

ESR スペクトルの測定は、日本電子製 FE1X を使い、X band, 9.2GHz, 22℃にて行った。得られたスペクトルより、スペクトルの分離幅、3本のシグナル強度、中央のシグナルの線幅を以前の論文に準じて計測した²⁾。マイクロ波の

出力は1mWとし、その他の測定条件は以下の様に設定した。
scan width : 330±5 mT, sweep time: 4 min, modulation : 100
kHz, 0.08 mT, amplitude: 2×100, response: 0.1 sec

4. ESR パラメーターの計算方法

ニトロキシドラジカルの配向や、異方的回転を示すオーダーパラメーター (以下 S) およびスピララベル剤の回転運動の速さを示す回転相関時間 (以下 τ) は得られたスペクトルより以前の論文に記載した計算式を用いて計算した^{2,13,14}。

III. 結 果

1. MLV の ESR スペクトルについて

5-DSA でラベルされた MLV のスペクトル (Fig. 2) は SDS 水溶液中のスペクトルに比べ 3 本のシグナルのうち低磁場および高磁場のシグナル強度が中央のシグナルに対して小さく、またスペクトルの分離幅が広がった。このことはラジカルの運動に異方性があり、回転運動の速度が遅いことを示している。16-DSA でラベルされた MLV のスペクトル (Fig. 2) は SDS 水溶液中のスペクトルに比べるとシグナル全体、特に高磁場側のシグナル強度が減少し、PC リポソームの方が SDS ミセルよりも運動が遅いことを示した。一方、PC リポソームで 5-DSA と 16-DSA を比べると、16-DSA をラベルした MLV のスペクトルは 5-DSA をラベルした MLV に比べ比較的鋭いシャープな 3 本のシグナルを示した。

臨床濃度の100倍量 (エーテルは20倍量) の麻酔薬を添加したところ、5-DSA でラベルした標本はセボフルレン、イソフルレン、ハロタン、エーテル、エタノールでは麻酔薬を添加していないコントロールに比べて中央および高磁場側のシグナルのスペクトル強度が9-45%増加したが、プロポフォール、サイアミラルではスペクトルに変化が見られなかった。

16-DSA においては、エタノールでスペクトル強度が増加した。セボフルレン、イソフルレン、ハロタン、エーテル、サイアミラルではスペクトル強度がわずかに増加したのみであった。プロポフォールではスペクトルに変化が見られなかった。

次に、5-DSA および 16-DSA について得られた ESR スペクトルより算出した S と τ の値を Table 1 にまとめた。なお、S を計算するにあたり、5-DSA でラベルしたスペクトルは S/N 比を上げるために、4 回積算したスペクトルにて計算した。5-DSA のスペクトルの線形は τ が 10^{-9} sec よりも遅いことを示しており、5-DSA 系の τ は算出できなかった。

5-DSA のコントロールにおける S は 0.67-0.69 であり、SDS 水溶液の場合の値 0.07-0.09 に比べ著しく増大しており、SDS 水溶液より異方性が大きく、回転運動の速さが

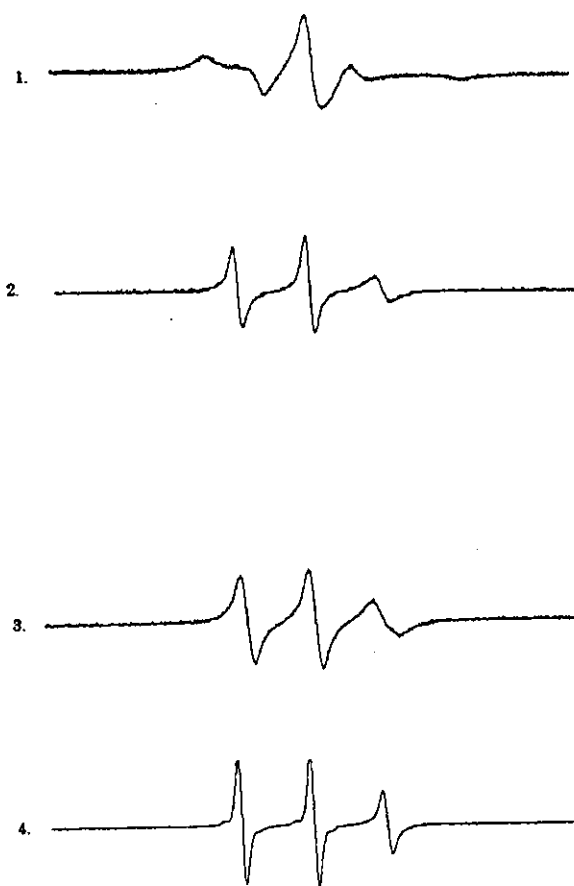


Fig. 2 ESR spectra of multilamellar vesicle (MLV) labeled with 5-DSA and 16-DSA.

1: ESR spectrum of MLV labeled with 5-DSA, 2: ESR spectrum of 5-DSA in SDS solution, 3: ESR spectrum of MLV labeled with 16-DSA, 4: ESR spectrum of 16-DSA in SDS solution.

The spectra of vesicles that are composed by phosphatidylcholine and labeled with 5-DSA suggest that the movement of the radicals is more anisotropic and the speed of the rotation is slower than that in SDS solution.

The spectra of vesicles labeled with 16-DSA show three sharp signals compared with 5-DSA.

遅くなったことを示した。イソフルレン、ハロセン、エーテル、エタノールを加えたところ、S は 0.03-0.04 減少した。一方、セボフルレン、プロポフォール、サイアミラルではほとんど変化しなかった。

16-DSA のコントロールにおける S は 0.13-0.15 と 5-DSA より著しく小さい値を示した。SDS 水溶液の値 0.03-0.07 と比べると 0.1 程度増大した。エタノールの添加により、S は 0.04 減少したが、セボフルレン、イソフルレン、ハロセン、エーテル、プロポフォール、サイアミラルではほとんど変化しなかった。

16-DSA の τ はコントロールでは約 40 psec であるが、セボフルレン、イソフルレン、ハロセン、エーテル、エタノールでは 5-8 psec 減少した。一方、プロポフォールでは変化

せず、サイアミラルでは 4 psec 増加した。

2. SUV の ESR スペクトルについて

5-DSA および 16-DSA のスペクトルの線形や強度は MLV 系と比較して大きな変化はなかった。麻酔薬を添加したところ、5-DSA においてハロタン、エーテル、エタノールではスペクトル強度がコントロールに比べ19-50%増加し、ラジカルの可動性がより高くなったことを示したが、セボフルレン、イソフルレン、プロポフォル、サイアミラルではスペクトルに変化が見られなかった。16-DSA においては、エタノールでスペクトル強度がコントロールに比べ41%増加した。セボフルレン、イソフルレン、ハロセン、エーテル、プロポフォルにおいてもスペクトル強度が増加したがその変化量は少なく15%未満であっ

た。

次に、5-DSA および 16-DSA について得られた ESR スペクトルより算出した S と τ の値を Table 2 にまとめた。5-DSA におけるコントロールの S は 0.65-0.68 であり、MLV の値と比較すると、SUV の方が 0.01-0.04 程度小さいか変化しなかった。麻酔薬を添加した際の S の変化をみると、S はコントロールに比べ、ハロセン、エタノールにて 0.03-0.06 減少した。一方、セボフルレン、イソフルレン、エーテル、プロポフォルでの変化は 0.02 以下だった。一方、サイアミラルでは 0.03 増加した。

16-DSA のコントロールにおける S は 0.11-0.16 と MLV の際と同様に 5-DSA より著しく小さい値を示し、また MLV の値と比較すると 0.02-0.03 小さかった。ハロセンの添加により S は 0.03 減少し、サイアミラルの添加にて S

Table 1 Order parameter S and rotational correlation time τ calculated from the ESR spectra of MLV labeled with 5-DSA and 16-DSA.

S values of control in MLV labeled with 5-DSA were bigger than that in SDS solution (S value is 0.07-0.09). This suggested that the movement of radicals in MLV is more anisotropic and that the speed of the rotation is slower. S values decreased when isoflurane, halothane, ether and ethanol were added, but remained unchanged when sevoflurane, propofol, and thiamylal were added.

S values of control in MLV labeled with 16-DSA were much smaller than that labeled with 5-DSA, and bigger than that in SDS solution labeled with 16-DSA (0.03-0.07). S values decreased when ethanol was added, but remained unchanged when anesthetics, except for ethanol, were added. τ values did not change by the addition of any kinds of anesthetics.

MLV	S				τ (10^{-12} S)	
	5 DSA		16 DSA		16 DSA	
	control	a hundredfold concentration	control	a hundredfold concentration	control	a hundredfold concentration
sevoflurane	0.69	0.67	0.14	0.13	42	34
isoflurane	0.69	0.66	0.14	0.12	41	33
halothane	0.68	0.64	0.13	0.11	38	31
ether	0.69	0.66*	0.14	0.12*	37	32
EtOH	0.67	0.63	0.15	0.11	39	32
propofol	0.69	0.69	0.15	0.15	36	37
thiamylal	0.68	0.69	0.14	0.16	40	44

*: twentyfold concentration

Table 2 Order parameter S and rotational correlation time τ calculated from the ESR spectra of SUV labeled with 5-DSA and 16-DSA.

The results were similar with those obtained with MLV as shown in Table 1.

SUV	S				τ (10^{-12} S)	
	5 DSA		16 DSA		16 DSA	
	control	hundredfold concentration	control	hundredfold concentration	control	hundredfold concentration
sevoflurane	0.66	0.67	0.12	0.12	45	41
isoflurane	0.67	0.65	0.13	0.12	46	41
halothane	0.68	0.62	0.13	0.10	43	32
ether	0.67	0.66*	0.12	0.12*	44	36
EtOH	0.66	0.63	0.13	0.11	43	32
propofol	0.65	0.67	0.13	0.12	44	48
thiamylal	0.66	0.69	0.13	0.16	48	42

*: twentyfold concentration